Influence of Surface Viscosity on Two-Dimensional Faraday Waves

Sebastián Ubal,[†,‡] María D. Giavedoni,[*,†] and Fernando A. Saita[†]

Instituto de Desarrollo Tecnológico para la Industria Química, CONICET - Universidad Nacional del Litoral, Güemes 3450, 3000 Santa Fe, Argentina, and Facultad de Ingeniería, Universidad Nacional de Entre Ríos, Ruta Prov. No. 11 KM 10, 3101 Oro Verde, Entre Ríos, Argentina

The onset for the formation of two-dimensional Faraday waves in a liquid with a viscous surface is numerically studied. The viscous behavior of the interface due to the presence of an insoluble surfactant, affects the surface traction and this, in turns, induces changes in the flow field. It is shown that the formation of waves of a given wavenumber in the absence of elastic effects requires a force that when plotted versus the Boussinesq number increases, producing a sigmoid curve. A detailed analysis of the interfacial variables and flow fields is carried out in order to understand this behavior.

1. Introduction

When a liquid lying on a flat solid surface is subjected to a vertical oscillatory motion, standing waves may appear at the free surface. The conditions for the formation of the waves depend on the physical chemistry properties of the liquid and on the frequency and amplitude of the imposed vibrations, as well as on the depth of the fluid layer. Faraday,[1] who was the first to investigate this phenomenon experimentally, also reported that the frequency of the standing waves was one-half the frequency of the external oscillation.

The study of free surface waves in a oscillating container is of great interest in many natural phenomena and engineering applications involving fluid mixing and fluid sloshing produced by the motion of the container. For instance, this phenomenon is important in the transportation and storage of liquids in vessels exposed to vibrations induced by the motion of the carrier or by earthquakes. Another application is the atomization of liquids, an important process to produce a large transfer area between a gas and a liquid. Examples of these operations are the humidification of air in air-conditioning plants and the atomization of fuel in diesel engines. The formation of the drops occurs when the oscillation imposed to the system produces a motion so intense that the amplitude of the surface waves becomes very large and part of the liquid is ejected toward the gas phase. In this case, the size of the drop—which depends on the excitation frequency—is a relevant feature because its diameter is inversely related to the transfer area. The above considerations show the importance of being able to predict the generation of resonant waves at a gas−liquid interface.

Even though the literature about Faraday waves is extensive (for an overview, see Miles and Henderson;[2] Miles;[3] and Perlin and Schultz[4]), only a few studies consider the influence of a surface active solute on this problem. When a surfactant is adsorbed on the interface, the surface tension is changed and the free surface may exhibit viscous properties; thus, the affected interfacial balance of stresses modifies the motion of the liquid in the bulk and the conditions for the formation of the waves. Very recently, Kumar and Matar[5−7] presented a full linear stability analysis of the Faraday problem when the free surface is covered by an insoluble surfactant. They assumed that surface tension is a linear function of the interfacial concentration of solute and that there are no stresses due to surface viscosity. The results presented by Kumar and Matar, valid for liquid layers of arbitrary viscosity and depth, show the dependence of the amplitude of the critical external acceleration and critical wavenumber on the Marangoni parameter. In two previous works[8,9] we numerically investigated the influence of the Marangoni forces on the formation of two-dimensional Faraday waves in a viscous fluid layer that is vibrated at 100 Hz and is covered by an insoluble surfactant. The equations solved in the bulk are Navier−Stokes and continuity equations with their appropriate boundary conditions, which include the interfacial mass balance of the surface active agent. In the first of those articles, surface tension is considered a linear function of the local concentration of surfactant, whereas in the second one, a nonlinear equation of state for the surface tension is employed, and its influence on the onset and evolution of the waves is analyzed.

As mentioned above, the adsorption of a surfactant along the interface not only affects the surface tension but also gives rise to surface shear and dilatational viscosities. The brief review presented in the previous paragraphs shows that the way in which surface viscosity affects the formation of Faraday waves has received almost no attention in the literature; therefore, the main goal of this work is to study the influence of this property. However, the following simplifying assumptions are made: (i) elastic effects are neglected to avoid masking viscous effects, and (ii) shear and dilatational viscosities are regarded as constants; i.e., they do not depend on the concentration of the adsorbed surfactant.

The second assumption is made for two reasons. (a) When elastic effects are neglected in the computations, a very refined mesh is required to follow the large concentration gradients generated along the interface in the time steps previous to the formation of the standing wave. In such a case our computer resources will not allow us to obtain a reliable solution in a realistic computational time. (b) A linear stability analysis of the problem (not presented here) indicates

* To whom correspondence should be addressed. E-mail: madelia@ceride.gov.ar.
† CONICET - Universidad Nacional del Litoral.
‡ Universidad Nacional de Entre Ríos.

10.1021/ie049188b CCC: $30.25
Published on Web 01/25/2005

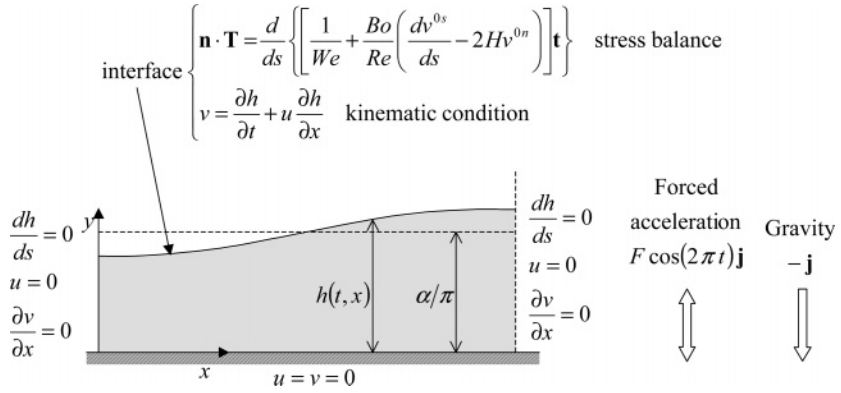

Figure 1. Sketch of the physical domain, summarizing the governing equations and boundary conditions.

that the contribution of the terms representing the interfacial viscosity dependence on surfactant concentration is of minor order. Because we are going to analyze the influence of surface viscosity on the stability limits, the behavior of the system should be similar whether we consider that contribution or not. Thus, the use of constant viscosity coefficients seems to be a reasonable assumption.

To reach our goal, we numerically solved the 2-D motion of a viscous liquid when a finite thickness film, covered with an insoluble surfactant, is subjected to a vertical oscillatory motion. The numerical technique employed is based on the finite element method for the spatial discretization of the governing equations and boundary conditions and on a finite difference scheme to march in time. This technique has already proved to be suitable to solve unsteady free surface flow problems with and without the presence of a surface active agent.[8,10]

The work is organized as follows. In Section 2, the governing equations with their boundary conditions are presented. Section 3 contains the main features of the numerical technique employed to solve the problem. In Section 4 the numerical solutions are presented and discussed, and finally, in Section 5, some concluding remarks are formulated.

2. Mathematical Model

A Newtonian and incompressible liquid with constant viscosity (μ) and density (ρ) lies on a horizontal plate that is vertically vibrated with angular frequency ω and amplitude a_0. The thickness of the liquid layer at rest measured along the y-coordinate is equal to H_0 and the air above it is regarded as inviscid. A monolayer of an insoluble surface active agent is covering the gas−liquid interface and is responsible for the viscous properties presented by the free surface.

To study the stability of the system, we perturb the liquid layer with a disturbance characterized by a wavenumber k and a very small amplitude ϵH_0 ($\epsilon \ll 1$), and we follow its evolution with time. This initial perturbation is described by

$$h(0, x) = \alpha/\pi[1 - \epsilon \cos(\pi x)],\ 0 \le x \le 1 \qquad (1)$$

where $h(t, x)$ is the liquid thickness and α is the dimensionless wavenumber. The characteristic scale adopted for length is one-half the wavelength of the initial disturbance ($\pi/k = \pi H_0/\alpha$). Since we are considering two-dimensional waves, the fluid height is a function of time and one spatial coordinate.

As illustrated in Figure 1, the reference frame is attached to the oscillating wall; therefore, the periodic acceleration induced to the liquid is added to gravity, and the governing equations in the bulk, that is Navier−Stokes and continuity equations, in dimensionless form result

$$\frac{\partial \mathbf{v}}{\partial t} + \mathbf{v}\cdot\nabla\mathbf{v} = -\nabla p + \frac{1}{Re}\nabla\cdot[\nabla\mathbf{v} + (\nabla\mathbf{v})^T] + \frac{1}{Fr}[F\cos(2\pi t) - 1]\mathbf{j} \qquad (2)$$

$$\nabla\cdot\mathbf{v} = 0 \qquad (3)$$

In eq 2, $Re = \rho\omega\pi H_0^2/2\mu\alpha^2$ is the Reynolds number, $Fr = \omega^2 H_0/4\pi\alpha g$ is the Froude number, and $F = a_0\omega^2/g$ is the forcing parameter that measures the ratio between the external acceleration and gravity. In addition to the characteristic length previously defined, time is scaled with $2\pi/\omega$, velocities are scaled with $\omega H_0/2\alpha$, and stresses are scaled with $\rho(\omega H_0/2\alpha)^2$. In the reference frame adopted, the boundary conditions for eqs 2 and 3 are those summarized in Figure 1 where u and v are the x- and y- components of the velocity, respectively.

The liquid adheres to the solid surface; therefore, the nonslip condition is imposed at the bottom wall. The extension of the domain along the x-axis is one-half the wavelength of the initial perturbation. Because we are interested in the formation of standing waves any wavy motion developed should be mirrored at both sides of the domain; in consequence, symmetry conditions are imposed at $x = 0$ and $x = 1$.

The boundary conditions at the free surface include the kinematic condition because the interface is a material surface; thus, we have

$$\frac{\partial h}{\partial t} + u\frac{\partial h}{\partial x} = v \qquad (4)$$

The monolayer of insoluble surfactant that covers the interface is responsible for the viscous properties presented by the free surface that in this work is modeled as Newtonian. Then, following Scriven[11] (see also Edwards et al.[12]), the surface stress tensor is $\mathbf{T}^{(S)} = [\sigma + (\kappa^{(S)} - \mu^{(S)})\ \nabla_{(S)}\cdot\mathbf{v}^{(S)}]\ \mathbf{I}^{(S)} + 2\ \mu^{(S)}\ \mathbf{D}^{(S)}$, where $\mathbf{I}^{(S)} = \mathbf{I} - \mathbf{nn}$ is the surface identity tensor, $\mathbf{n}$ is the external unit normal to the interface, σ is the surface tension, $\kappa^{(S)}$ and $\mu^{(S)}$ are the surface dilatational and shear viscosity coefficients, respectively, $\nabla_{(S)} = \mathbf{I}^{(S)}\cdot\nabla$ is the surface gradient operator, $\mathbf{v}^{(S)}$ is the surface velocity, and $\mathbf{D}^{(S)} = [\nabla_{(S)}\mathbf{v}^{(S)} + (\nabla_{(S)}\mathbf{v}^{(S)})^T]$ is the rate of the surface strain tensor. Since we are only dealing with two-dimensional

waves, the surface stress tensor reduces to $\mathbf{T}^{(S)} = [\sigma + (\kappa^{(S)} + \mu^{(S)})\ \nabla_{(S)}\cdot\mathbf{v}^{(S)}]\ \mathbf{I}^{(S)}$. Furthermore, the following identities hold: $\nabla_{(S)} = \mathbf{t}\ d/ds$, $\nabla_{(S)}\cdot\mathbf{v}^{(S)} = dv^{0s}/ds - 2H\ v^{0n}$, and $\mathbf{I}^{(S)} = \mathbf{tt}$, where s is the arc-length measured from $x = 0$ toward $x = 1$, $\mathbf{t}$ is the unit tangent vector to the interface pointing toward increasing values of s, $2H$ is the mean curvature of the free surface, and $\mathbf{v}^{(S)} = v^{0s}\ \mathbf{t} + v^{0n}\ \mathbf{n}$ is the interfacial velocity. Under these conditions, the surface traction is given by

$$\mathbf{n}\cdot\mathbf{T} = \frac{d}{ds}\left\{\left[\sigma + (\kappa^{(S)} + \mu^{(S)})\left(\frac{dv^{0s}}{ds} - 2Hv^{0n}\right)\right]\mathbf{t}\right\} \quad (5)$$

As we have mentioned in the Introduction, the main goal of this work is to study the influence of surface viscosity on the onset of two-dimensional Faraday waves. Then, we neglect surface elasticity—i.e., surface tension is regarded as a constant— and we assume that the sole effect of the surfactant is to produce a viscous interface. Under these conditions, eq 5 can be written in dimensionless form as follows:

$$\mathbf{n}\cdot\mathbf{T} = \frac{d}{ds}\left\{\left[\frac{1}{We} + \frac{Bo}{Re}\left(\frac{dv^{0s}}{ds} - 2Hv^{0n}\right)\right]\mathbf{t}\right\} \quad (6)$$

where the same symbols used in eq 5 are here employed for the dimensionless variables. In eq 6, $Bo = (\kappa^{(S)} + \mu^{(S)})\alpha/\pi H_0\mu$ is the Boussinesq parameter that measures the ratio between surface and bulk viscosity, and $We = \pi\rho\omega^2 H_0^3/4\sigma\alpha^3$ is the Weber number. Then, the normal and tangential components of the surface traction are $T_{nn} = 2H\ [1/We + Bo/Re\ (dv^{0s}/ds - 2H\ v^{0n})]$ and $T_{nt} = d/ds[Bo/Re\ (dv^{0s}/ds - 2H\ v^{0n})]$, respectively. To analyze the effects of surface viscosity, it should be noticed that the quantity $dv^{0s}/ds - 2H\ v^{0n}$ represents the rate of deformation of the free surface, the first term is the surface stretching and the second one is the surface inflation. Therefore, surface viscosity introduces an extra term in the normal component of the traction that depends on the changes in surface area and gives rise to a nonzero tangential component when the free surface presents a nonhomogeneous deformation.

The next section describes the numerical procedure employed to solve the problem.

3. Numerical Technique

The set of governing eqs 2 and 3 with their boundary conditions was numerically solved using a procedure based on the Galerkin weighted residuals/finite element method for the spatial discretization of the problem. The time-marching scheme is a finite-difference second-order predictor/corrector. The moving interface is followed by means of an Arbitrary Lagrangian-Eulerian technique known as the spines method.[10] Since this methodology has been employed in several previous works, only its main features are described next. Further details concerning the numerical procedure can be found elsewhere.[8−10,13]

The physical domain (in the x-y plane) is tessellated into a structured mesh of nine-node quadrilaterals, which are isoparametrically mapped into the unit square (in the ξ-η plane, $0 \le \xi, \eta \le 1$). The primary unknowns are the velocity and pressure fields, and the free surface location; velocities and pressures are approximated by mixed interpolation: biquadratic basis functions ($\phi^k(\xi,\eta)$) are employed for the x- and y- velocity components and bilinear basis functions ($\psi^k(\xi,\eta)$) are employed for the pressure. In the spine technique the free surface height is approximated by a quadratic interpolation: $h(t,\xi) = \sum_{i=1}^{3} h^i(t)\hat{\phi}^i(\xi)$, with $h^i(t)$ being the time-dependent length measured along the i-th spine, that here is a straight line perpendicular to the solid wall. The spines form the lateral sides of the elements, while the other two sides automatically adjust to the shape adopted by the free surface.

When the standard Galerkin weighting procedure is applied to eqs 2 and 3 and their boundary conditions, a system of nonlinear ordinary differential equations is obtained. The time-marching scheme employed to solve this system consists of a second-order predictor-corrector finite difference formulation.[14] The time derivatives are approximated by the trapezoid rule and the system of nonlinear algebraic equations obtained is solved by Newton iteration at each time step. This loop is initialized with the approximate solutions for velocities and free surface coefficients provided by an Adams−Bashforth predictor, while pressures are initially set to the value of the previous instant of time. The time-step size is adjusted according to the method of Crisfield[15] in order to meet the convergence criterion adopted (the mean square root of the error in the Newton loop must be smaller than 10^{-6}) in a predetermined number of iterations. At the end of this procedure, all the variables are simultaneously obtained for each time step.

3.1 Mesh Adoption. To obtain a proper representation of the flow field, the following criteria were used to adopt an appropriate finite element mesh: (i) the mesh is refined near the oscillating wall and in the vicinity of the free surface so that the boundary layers can be resolved, and (ii) the number of elements in the x-direction is adjusted to get an accurate description of the interfacial variables.

A mesh with 20 elements in the x- direction and 7 elements in the y- direction was found suitable for all the numerical experiments performed in this work. The results of some of the numerical tests carried out are illustrated in Figure 2. The tangential component of the surface traction as a function of x (Figure 2a) and the magnitude of the velocity vector at $x = 0.5$ (Figure 2b) are shown for two different tessellations and several instants of time along a cycle. These two variables were considered appropriate to determine the quality of the mesh; the first one because it depends directly on surface viscosity and the second one because it is useful to analyze the flow at the boundary layers. The curves depicted in Figure 2a and b clearly show that a more refined mesh does not change the predictions.

4. Results

As previously mentioned, the properties of the interface can be largely modified when the free surface of a liquid layer is covered with an insoluble surfactant. This is particularly important for deforming interfaces because the concentration gradients of adsorbed surfactants associated with surface deformations give rise to local variations of interfacial properties. The aim of this work is to analyze the influence of surface viscosity on the formation of two-dimensional Faraday waves. Even though interfacial properties (σ, $\kappa^{(S)}$, and $\mu^{(S)}$) should depend on the interfacial concentration of surfactant, in this work we neglect this dependence, and assume that they are constant. Thus, in the system under study, the Marangoni traction is absent and the effect of the surfactant is just to produce nonzero surface viscosity

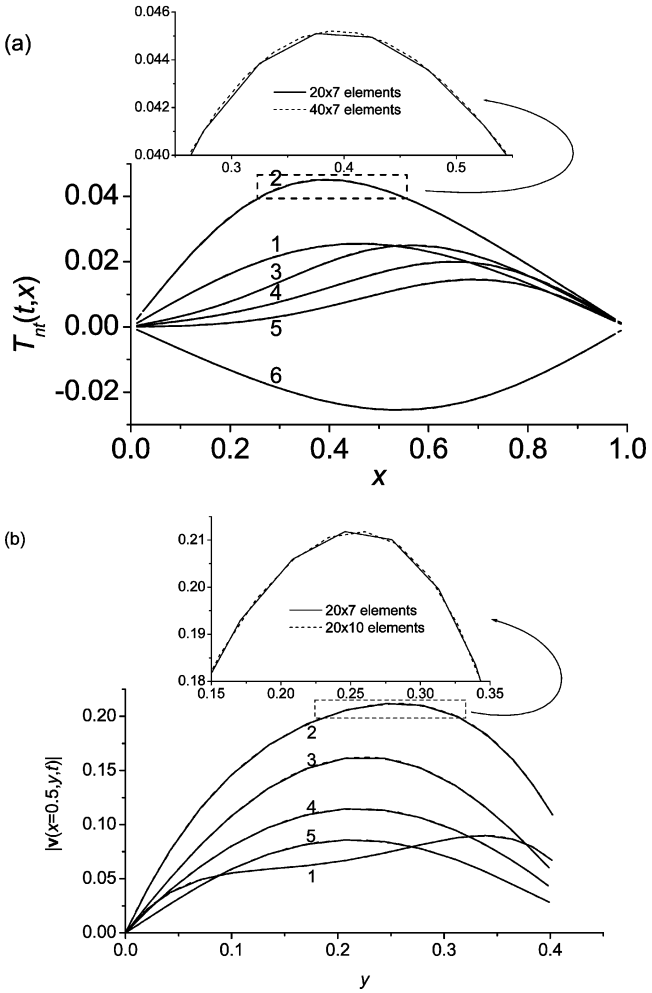

Figure 2. Mesh refinement tests. (a) Spatial distribution of the tangential component of the surface traction, and (b) magnitude of the velocity vector at $x = 0.5$, for several equally spaced instants of time along a cycle. The results pertain to $Re = 24.87$, $We = 2.818$, $Fr = 2.544$, $\alpha = 1.26$, $Bo = 1$, and $F = 15$.

coefficients. Consequently, in this Section results are presented as a function of the Boussinesq number which is the only dimensionless parameter required to describe the influence of the surface active agent.

An important issue in this problem is to detect the minimum force required to form waves of a particular wavenumber. We expect the value of this force to be affected by the viscous properties of the interface; to study how it depends on the Boussinesq number we performed numerical experiments in which the value of this parameter was widely varied. With this purpose, we first defined a reference case (*RC*) characterized by $Bo = 0$, the other parameters being as follows

$$\alpha^2\, Re = 39.478,\ \alpha^3\, We = 5.6375,\ \alpha\, Fr = 3.206$$

This particular set of dimensionless numbers corresponds to typical values of the physicochemical properties of the system:

$$\rho = 1000\ \mathrm{kg/m^3},\ \mu = 0.025\ \mathrm{Pa\ s},\ \sigma_0 = 0.055\ \mathrm{N/m},\ H_0 = 10^{-3}\ \mathrm{m},\ \omega = 200\,\pi\ \mathrm{s^{-1}}$$

To complete the characterization of the *RC*, a particular value of the wavenumber was selected. In this work, α was fixed equal to α_C, that is the wavenumber

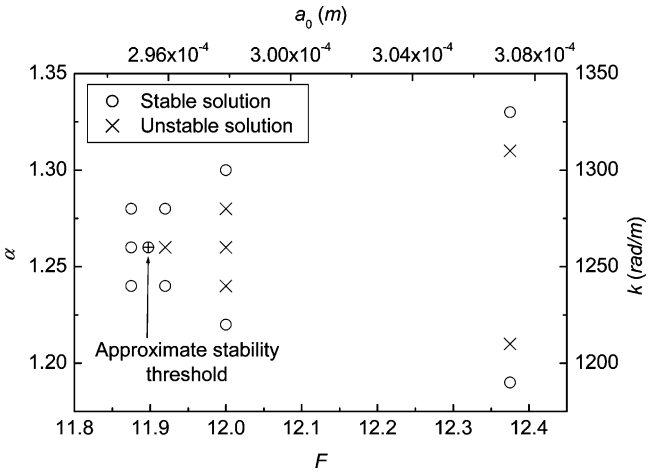

Figure 3. Stability map in the F-α plane for $Bo = 0$, $\alpha^2\, Re = 39.478$, $\alpha^3\, We = 5.6375$, $\alpha\, Fr = 3.206$.

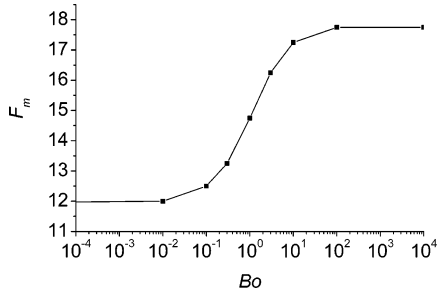

Figure 4. Minimum vibration force (F_m) vs Bo. The other parameters of the system have the same value as in *RC*.

corresponding to the onset of the instability when interfacial viscous effects are absent. The critical conditions were detected by constructing the stability map shown in Figure 3. Every point in this chart represents the outcome of a single simulation starting with the free surface slightly perturbed according to eq 1 with $\epsilon = 0.001$ and the liquid at rest. Crosses denote unstable cases (the initial amplitude of the oscillation does not decay to zero along the computation), while circles indicate stable ones (the initial amplitude of the oscillation decays to zero along the computation).

An unstable region can be clearly distinguished in Figure 3, where the solutions are characterized by a subharmonic motion of a surface wave with a length equal to twice the extension of the computational domain. The threshold conditions are indicated by the symbol $\oplus$, and they are approximately located at ($F_C = 11.9$, $\alpha_C = 1.26$). This particular wavenumber ($\alpha = \alpha_C = 1.26$) together with the values of the parameters indicated in Figure 3 defines the reference case employed in the numerical experiments performed to disclose the influence of the Boussinesq number.

4.1 Effect of Surface Viscosity on Stability Limits. The way in which surface viscosity affects the onset of the instability was studied by computing solutions with Bo varying between 0.01 and 10^4 or, equivalently, for $(\kappa^{(S)} + \mu^{(S)})$ between 0.623×10^{-3} sp and 623 sp (see refs 12 and 16); the values of the remaining dimensionless parameters being those defining the *RC*. From these computations—in which several values of F were explored for each Bo selected—we obtained the minimum acceleration (F_m) required to form waves with wavenumber α_C as a function of the Boussinesq number. Results are depicted in Figure 4 and they show that F_m presents a sigmoid behavior. In fact, results reported

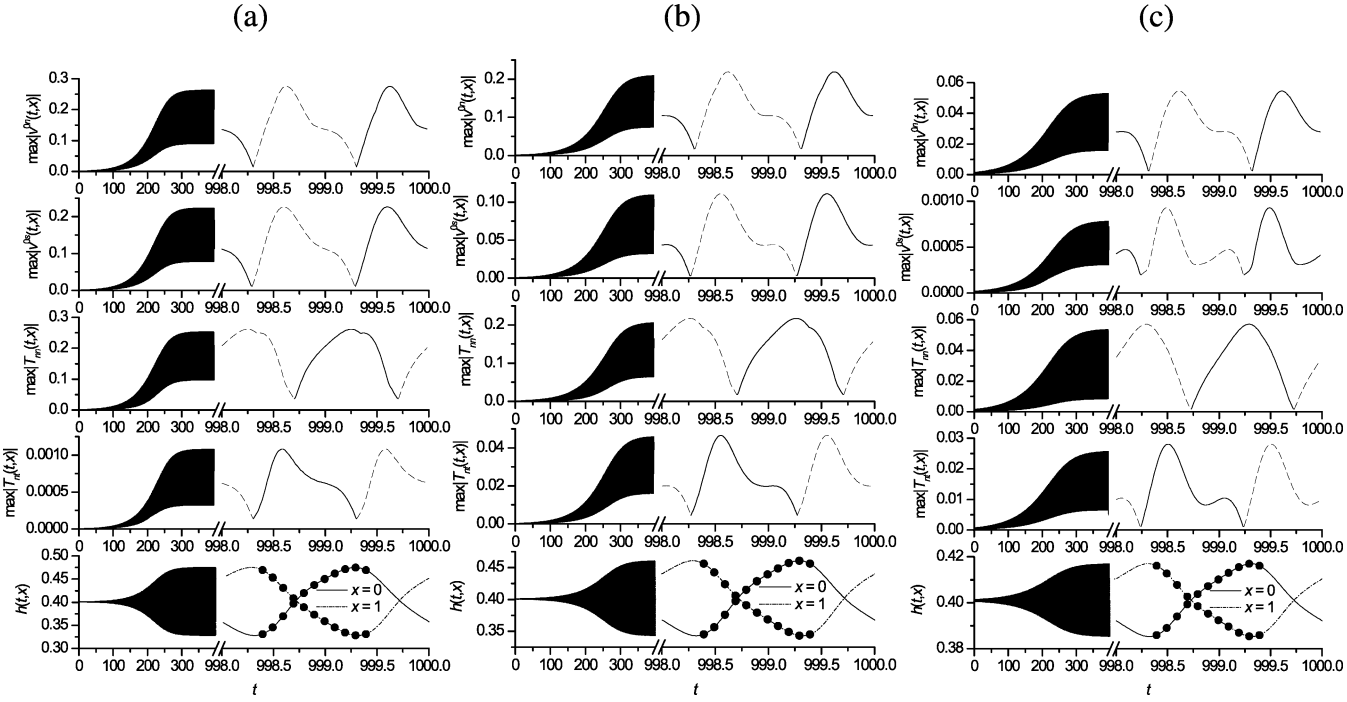

Figure 5. Temporal evolution of interfacial variables near the threshold for (a) ($Bo = 0.01$, $F = 12.25$), (b) ($Bo = 1$, $F = 15$), and (c) ($Bo = 100$, $F = 18$). From top to bottom, maximum absolute values of normal and tangential components of surface velocity, maximum absolute values of normal and tangential components of surface traction, and free surface position at the surface ends. The dots in the figures of the bottom row are equally spaced in time and are for future reference.

in this figure show that the larger variations of F_m occur in the neighborhood of $Bo = 1$, and that there are limiting values of the Boussinesq number beyond which viscous effects are not noticeable. Outside these bounds F_m remains almost constant ($Bo = 0.01$ and $Bo = 100$ in the present case). At $Bo = 1$, the minimum acceleration is about 1.25 times the critical acceleration required to form a wavy interface for a clean system, while for $Bo \geq 100$, F_m is 50% higher than the case without surface viscosity.

Interfacial viscosity not only modifies the normal component of the surface traction but also gives rise to a nonzero tangential component. Therefore, it is expected that the magnitude of the interfacial flow variables should depend on the Boussinesq number and that this dependence might be associated with the changes experienced by the minimum acceleration required to form waves as Bo is varied.

4.2 Time Variation of the Interfacial Variables. To gain further knowledge about the phenomena involved in the formation of the surface waves when surface viscosity is not negligible, the time evolution of several interfacial variables for some of the numerical experiments illustrated in Figure 4 is analyzed. The selected cases are $Bo = 0.01 - F = 12.25$, $Bo = 1 - F = 15$, and $Bo = 100 - F = 18$, and the corresponding results are illustrated in Figure 5a, b, and c, respectively. Each column of Figure 5 shows, from top to bottom, the maximum absolute values of the normal and tangential components of the surface velocity, the maximum absolute values of the normal and tangential components of the traction vector, and the liquid height at the free surface ends. In these figures, dashed lines are used to illustrate the evolution of the selected variables during one-half of the cycle.

A close inspection of the evolution of the interfacial variables in Figure 5 leads to the following conclusions: when Boussinesq varies between 0 and 1 the more sensitive variable is the tangential component of the interfacial traction (see Figure 5a and b), which is about 40 times larger for $Bo = 1$ than for $Bo = 0.01$. To a smaller extent, the tangential component of the surface velocity is reduced by almost one-half within the same range of Bo. On the other hand, when Bo is larger than 1 (see Figure 5b and c), the magnitude of both the surface velocity and the free surface deflection show that the motion of the system is slowed. In particular, there is a striking reduction of v^{0s} when the Boussinesq number varies between 1 and 100.

Another feature of the results reported in Figure 5 is that the liquid motions in the bulk and near the free surface are almost in phase (see the evolutions of $h(t, x = 0, 1)$ and v^{0n} and compare them with that of v^{0s}); this is in contrast with the phase shift associated with the elastic effects of an insoluble surfactant.[8,9]

To provide further details on the evolution of the interfacial variables, we analyze the spatial distribution of the free surface height, the normal and tangential components of the surface velocity, the rate of deformation of the free surface, and the tangential component of the interfacial traction along the free surface. These variables for selected instants of time along a cycle of the standing wave formed are illustrated in Figure 6 a−c, where curve 1 corresponds to the first instant of time marked with a dot in Figure 5, curve 2 corresponds to the third instant of time, and so on.

Results concerning $h(t, x)$ show that the oscillation amplitude of the free surface diminishes with Bo, and that the interface presents a sinusoidal shape along the whole cycle in all the cases considered. The distribution of the normal component of the surface velocity follows the free surface configuration. As expected, v^{0n} is nearly zero when the free surface amplitude is nearly maximum (curve 1), it is positive when the free surface moves upward, and negative otherwise (curves 2 to 5), and attains a maximum when the free surface is almost flat

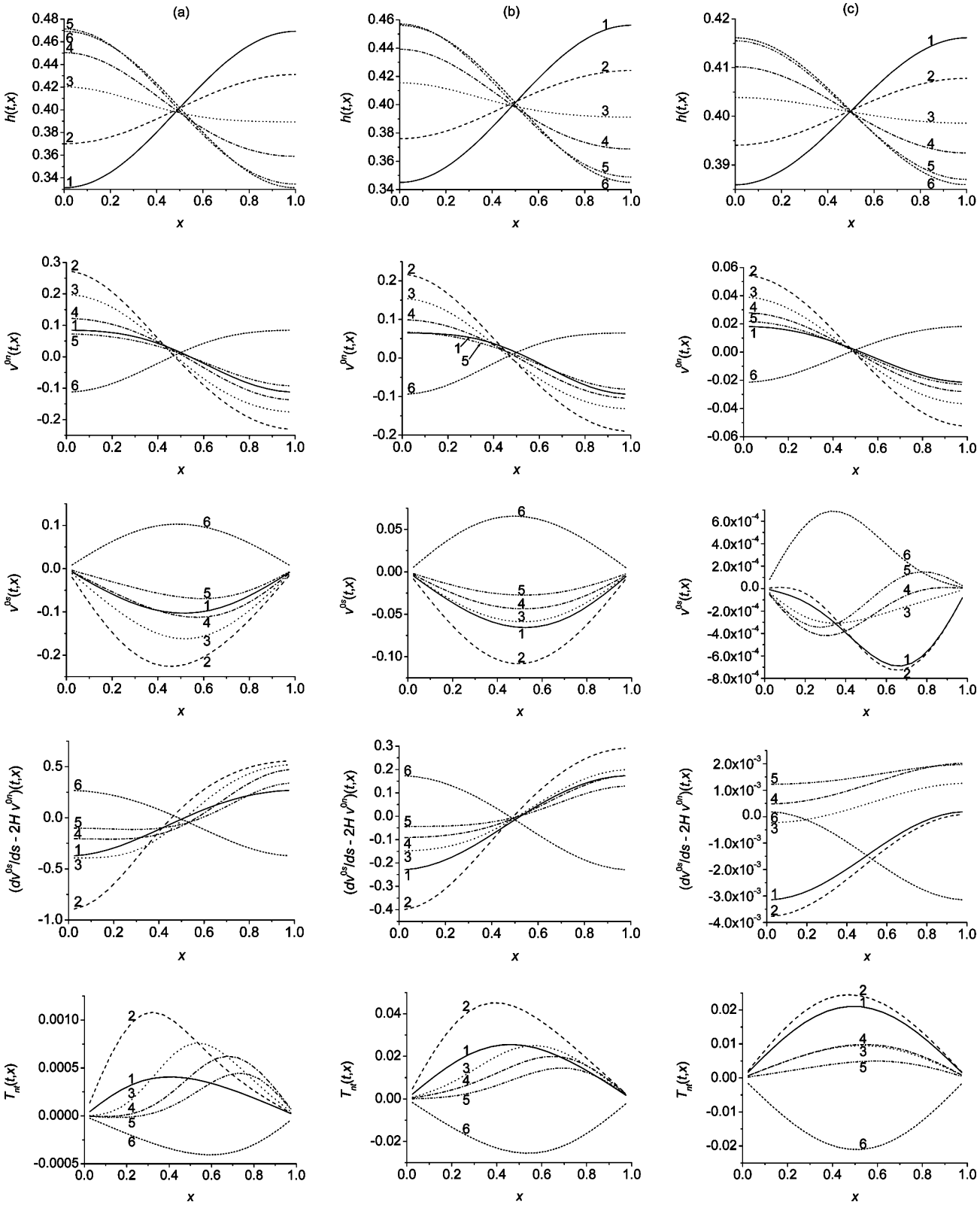

Figure 6. Temporal evolution of the spatial distribution of several interfacial variables at the stability limit for (a) (Bo = 0.01, F = 12.25), (b) (Bo = 1, F = 15), and (c) (Bo = 100, F = 18). From top to bottom, free surface height, normal and tangential components of the surface velocity, interfacial rate of strain, and tangential component of the interfacial traction. Curves 1−6 in each illustration correspond to every other instant of time marked with dots in Figure 5.

(see curve 2). Also, as we have already pointed out (see Figure 5), the magnitude of this variable diminishes with Bo, especially when this parameter changes between 1 and 100.

The distributions of v^{0s} during the cycle are quite similar for the two smaller values of Bo considered in this analysis. In fact, in both cases the distribution is nearly parabolic with the vertex located close to the midpoint of the computational domain; however, this variable is somewhat smaller for Bo = 1 than for Bo = 0.01. A radical change occurs for Bo = 100; in this case not only do the velocity profiles have an asymmetric

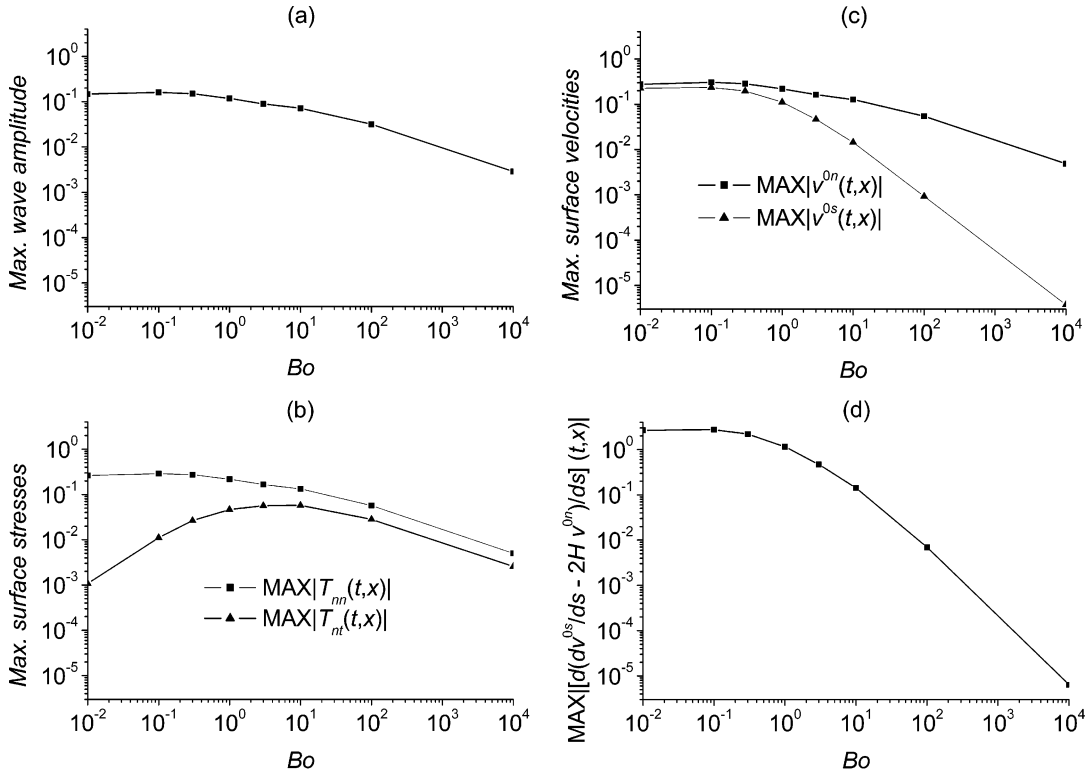

Figure 7. Maximum absolute values of the interfacial variables near the threshold as a function of the interfacial viscosity parameter. The other dimensionless numbers correspond to *RC*. (a) Wave amplitude, (b) surface stresses, (c) surface velocities, and (d) derivative of the rate of surface deformation.

shape but the surface velocity is also negligible during the whole cycle. From these illustrations it can be inferred that the derivative of the surface velocity along the interface diminishes when the Boussinesq number varies between 1 and 100; that is, the surface stretching diminishes with *Bo* and consequently, its contribution to the total deformation of the interface should also be smaller.

The rate of deformation of the free surface depends on the stretching, quantified by dv^{0s}/ds, and on the inflation, quantified by $2Hv^{0n}$. Results, reported in the fourth row of Figure 6, show that this variable becomes smaller as the interfacial viscosity increases and that it is almost negligible for a very viscous interface ($Bo = 100$). Moreover, these results together with those illustrated in the previous rows of this figure also point out that the rate of deformation is largely determined by the surface stretching, and that this quantity becomes negligible at large values of the Boussinesq number.

From a very simple calculation, it is easy to conclude that the normal component of the traction (eq 6) mostly depends on capillary effects, the contribution of the surface viscosity term being negligible. On the contrary, surface viscosity is responsible for the nonzero tangential component of the traction that opposes the nonuniform deformation of the free surface and, consequently, the motion of the fluid (see the third and last rows of Figure 6). Figure 6 shows that *Tnt* rapidly increases with *Bo* when this parameter is smaller than one indicating that v^{0s} and its derivatives diminish slower than the rate at which *Bo* is augmented. However, the opposite is true for larger values of *Bo*, and *Tnt* begins to decrease when the surface viscosity is augmented.

A more general picture of the influence of *Bo* can be obtained by examining how the interfacial variables change during a cycle. For that purpose Figure 7 portrays the maximum absolute values of the wave amplitude, the surface velocity, the traction, and the derivative of the rate of interfacial deformation along *s* versus *Bo*, for the cases already considered in Figure 4. Results illustrated in Figure 7 show that all these variables, except the tangential component of the traction, have similar trends: they slightly increase or remain constant in the range of *Bo* between 0.01 and 0.1 and they decline rapidly for larger values of this parameter (see Figure 7a−d). Since both capillary stresses and maximum amplitude of the surface wave are closely related to the magnitude of the normal component of the velocity, the similarity between these three curves is reasonable. A closer examination of this figure for *Bo* larger than 100 reveals that the wave amplitude, the two components of the surface traction, and the normal component of the interfacial velocity are approximately proportional to $Bo^{-1/2}$, while the tangential component of the surface velocity is proportional to Bo^{-1}.

The curves depicted in Figure 7c point out that the tangential component of the surface velocity decreases faster than the normal component, a result that was previously reported in this section. From this figure, it can be noticed that the ratio between $MAX|v^{0n}|$ and $MAX|v^{0s}|$ is approximately equal to 2, 9, 60, and 1300 when the Boussinesq number is equal to 1, 10, 100, and 10^4, respectively. Results not reported here show that the contributions of the surface stretching (dv^{0s}/ds) and the surface inflation ($2Hv^{0n}$) to the total rate of surface deformation are of the same order when $Bo \geq 100$; moreover, within this range of the Boussinesq param-

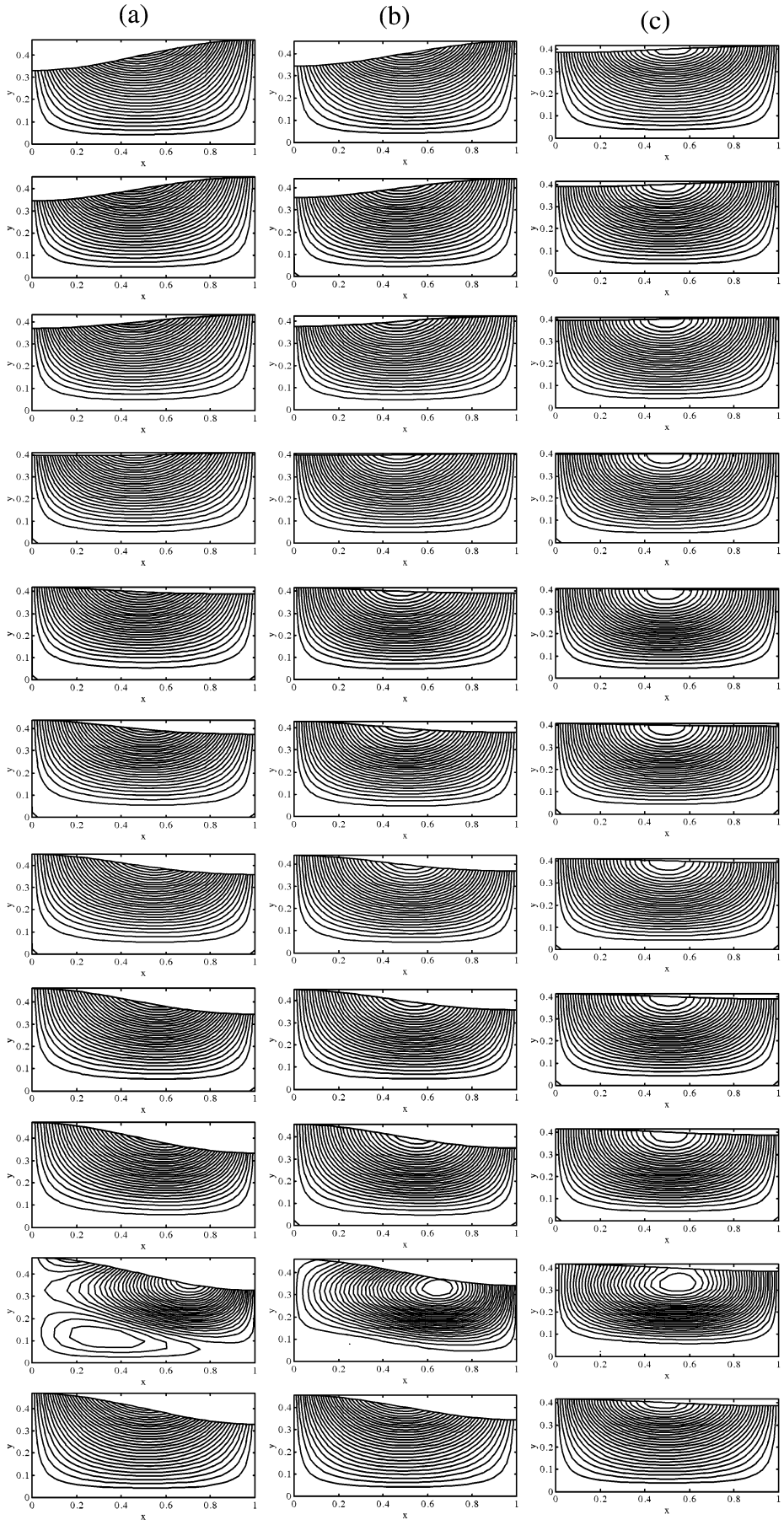

Figure 8. Temporal evolution of the streamlines near the threshold for *RC* and (a) ($Bo = 0.01$, $F = 12.25$), (b) ($Bo = 1$, $F = 15$), and (c) ($Bo = 100$, $F = 18$). Time advances from top to bottom, according to the instants of time marked with dots in Figure 5.

eter both quantities are nearly inversely proportional to *Bo*. Since the tangential component of the surface stress decays with $Bo^{-1/2}$, it can be concluded (see eq 6) that the derivative of the rate of deformation along the tfree surface must be approximately proportional to $Bo^{-3/2}$, as it is shown in Figure 7d. Thus, the rate of interfacial deformation rapidly tends to become uniform as the Boussinesq number is augmented, a result also suggested in the fourth row of Figure 6.

The graph corresponding to $MAX|T_{nt}|$ vs *Bo* is somewhat different. At first, a larger value of *Tnt* is associated with the presence of a more viscous interface; in fact, results reported in Figure 7b show that $MAX|T_{nt}|$ rapidly increases until it attains a maximum near $Bo = 10$. Nevertheless, if the surface viscosity is too high, an increment of this property will produce a smaller value of the tangential component of the traction. Having in mind that *Tnt* is the product of *Bo* times the derivative of the rate of surface deformation the trend followed by this variable becomes evident: Figure 7d shows that the rate of surface strain is fairly constant when *Bo* is smaller than one, and that it decreases rapidly—approximately as $Bo^{-3/2}$—when *Bo* is larger than 10; therefore, the product (i.e., T_{nt}) should vary as *Bo* and as $Bo^{-1/2}$ when this parameter is small and large, respectively. The curves portrayed in Figure 7b show that the two components of the surface stress decrease with a very similar slope, $MAX|T_{nn}|$ being approximately equal to $2MAX|T_{nt}|$ for $Bo \geq 100$.

When results illustrated in Figures 7 and 4 are considered together, the following conclusions can be drawn. At values of *Bo* smaller than one the increase of surface viscosity has little effects on the interfacial variables, except for the tangential interfacial stress that augments almost linearly with *Bo*. Since this is the only noticeable change observed, it is understandable that an increasing applied force would be needed to keep the unstable waves when the interface becomes more viscous. However, when the value of *Bo* is close to 10 the behavior of the system changes completely: the tangential interfacial velocity rapidly diminishes with interfacial viscosity and the rate at which the applied force has to increase to maintain the unstable waves is reduced. Thus, at about $Bo = 100$ a point is reached where the tangential velocities are negligible and the velocity field becomes perpendicular to the interface. It seems that once this occurs, an increase of surface viscosity cannot produce further qualitative changes in the flow field and the critical excitation F_m becomes constant as reported in Figure 4.

The influence of the Boussinesq number on the velocity field can be better understood by analyzing the streamlines depicted in Figure 8, corresponding to $Bo = 0.01 - F = 12.25$, $Bo = 1 - F = 15$, and $Bo = 100 - F = 18$. The selected instants of time are equally spaced and correspond to those marked with dots in the last row of Figure 5. The pictures portrayed in Figure 8 clearly show that the streamlines near the surface are closer to each other for the lowest value of *Bo* (Figure 8a). They come apart as *Bo* becomes larger (Figure 8b and c) indicating that the motion of the liquid in the vicinity of the interface is relatively less important when the free surface is very viscous. Also, the streamlines gradually become more perpendicular to the interface when *Bo* is augmented in agreement with the results previously presented. Finally, these illustrations and those presented in Figure 5 confirm that the motions of the liquid in the bulk and along the free surface are almost in phase.

5. Final Remarks

In this work a mathematical model of a Newtonian liquid film with uniform interfacial viscosity subjected to an oscillatory vertical movement of constant frequency is presented and numerically solved. The numerical technique employed is based on the finite element method and a suitable parametrization of the free surface to simultaneously resolve the system of governing equations at each time step. The time-marching scheme made use of a second-order predictor-corrector technique applied with a finite difference formulation.

The results obtained show, for waves of a particular length, how the minimum imposed acceleration has to be increased to keep the induced standing waves when the surface viscosity is augmented. The predictions indicate that the applied force follows a sigmoid curve with a minimum value for a clean interface; i.e., with no interfacial viscosity, and a maximum when the interfacial viscosity is large enough so that the interfacial tangential motions result strongly restricted. Moreover, the information provided by the numerical technique about the interfacial variables and flow fields for the different values of the Boussinesq parameter considered helps to understand the trend followed by F_m vs *Bo*.

Though the cases analyzed only consider a uniform value of the interfacial viscosity, results of a linear stability analysis—not yet published—indicate that contributions of the terms representing the interfacial viscosity dependence on surfactant concentrations are of minor order.

Acknowledgment

This research has been supported by the Universidad Nacional del Litoral, CONICET and the ANPCyT.

Nomenclature

Dimensionless Groups

Bo = Boussinesq number, $(\mu^{(S)} + \kappa^{(S)})\alpha/\pi\mu H_0$.
F = ratio between the external acceleration and gravity, $a_0\omega^2/g$.
Fr = Froude number, $\omega^2 H_0/4\pi\alpha g$.
Re = Reynolds number, $\rho\omega\pi H_0^2/2\mu\alpha^2$.
We = Weber number, $\pi\rho\omega^2 H_0^3/4\sigma\alpha^3$.

Latin Symbols

a_0 = amplitude of the external vibration (m).
H = dimensionless mean surface curvature.
H_0 = thickness of the liquid layer at rest (m).
h = dimensionless liquid height.
k = wavenumber (m^{-1}).
$\mathbf{n}$ = outward unit vector normal to the free surface.
p = dimensionless pressure.
s = arc length measured from $x = 0$ toward $x = 1$.
$\mathbf{T}$ = stress tensor (N m^{-2}).
T_{nn} = normal component of the surface traction.
T_{nt} = tangential component of the surface traction.
t = dimensionless time.
$\mathbf{t}$ = unit tangent vector to the free surface.
u = x-component of the velocity vector.
v = y-component of the velocity vector.
$\mathbf{v}$ = dimensionless velocity vector.

v^{0n} = normal component of the interfacial velocity.
v^{0s} = tangential component of the interfacial velocity.

Greek Symbols

α = dimensionless wavenumber.
$\kappa^{(S)}$ = surface shear viscosity (kg s^{-1}).
μ = liquid viscosity (kg m^{-1} s^{-1}).
$\mu^{(S)}$ = surface dilatational viscosity (kg s^{-1}).
ρ = liquid density (kg m^{-3}).
σ = surface tension (N m^{-1}).
ω = angular frequency of the external vibration (s^{-1}).

Literature Cited

(1) Faraday, M. On the forms and states assumed by fluids in contact with vibrating elastic surfaces. *Philos. Trans. R. Soc. London* **1831**, *121*, 319.

(2) Miles, J.; Henderson, D. Parametrically forced surface waves. *Annu. Rev. Fluid Mech.* **1990**, *22*, 143.

(3) Miles, J. On Faraday waves. *J. Fluid Mech.* **1993**, *248*, 671.

(4) Perlin, M.; Schultz, W. W. Capillary effects on surface waves. *Annu. Rev. Fluid Mech.* **2000**, *32*, 241.

(5) Kumar, S.; Matar, O. K. Parametrically driven surface waves in surfactant-covered liquids. *Proc. R. Soc. London A* **2002**, *458*, 2815−2828.

(6) Kumar, S.; Matar, O. K. On the Faraday instability in a surfactant-covered liquid. *Phys. Fluids* **2004**, *16*, 39.

(7) Kumar, S.; Matar, O. K. Erratum: "On the Faraday instability in a surfactant-covered liquid" [*Phys. Fluids* **2004**, *16*, 39]. *Phys. Fluids* **2004**, *16* (8), 3239.

(8) Ubal, S.; Giavedoni, M. D.; Saita, F. A. Elastic effects of an insoluble surfactant on the onset of two-dimensional Faraday waves: A numerical experiment. *J. Fluid Mech.* **2005**, *524*, 305−329.

(9) Ubal, S.; Giavedoni, M. D.; Saita, F. A. The formation of Faraday waves on a liquid covered with an insoluble surfactant: influence of the surface equation of state. *Lat. Am. Appl. Res.* **2005**, 35, 59−66.

(10) Kheshgi, H. S.; Scriven, L. E. Penalty finite elements analysis of unsteady free surface flows. In *Finite Element in Fluids*; Gallagher, R. H., Oden, J. T., Eds.; John Wiley & Sons Ltd.: New York, 1984; Vol. 5, Ch. 19, p 393.

(11) Scriven, L. E. Dynamics of a fluid interface. *Chem. Eng. Sci.* **1960**, *12*, 98.

(12) Edwards, D. A.; Brenner, H.; Wasan, D. T. *Interfacial Transport Processes and Rheology*; Butterworth-Heinemann: Boston, MA, 1991.

(13) Ubal, S.; Giavedoni, M. D.; Saita, F. A. A numerical analysis of the influence of the liquid depth on two-dimensional Faraday waves. *Phys. Fluids* **2003**, *15* (10), 3099.

(14) Gresho, P. M.; Lee, R. L.; Sani, R. L. On the time-dependent solution of the incompressible Navier−Stokes equations in two and three dimensions. In *Recent Advances in Numerical Methods in Fluids*; Taylor, C., Morgan, K., Eds.; Pineridge Press: Swansea, U.K., 1979; Vol. 1, Ch. 2, p 27.

(15) Crisfield, M. A. A fast incremental iterative solution procedure that handles "snap through". *Comput. Struct.* **1981**, *13*, 55.

(16) Miller, R.; Wüstneck, R.; Krägel, J.; Kretzschmar, G. Dilatational and shear rheology of adsorption layers at liquid interfaces. *Colloids Surf., A* **1996**, *111*, 75.

Received for review August 31, 2004
Revised manuscript received December 9, 2004
Accepted December 9, 2004

IE049188B